Hindawi
Advances in Civil Engineering
Volume 2018, Article ID 1053232, 13 pages
https://doi.org/10.1155/2018/1053232

Research Article

Determining Time Variation of Cable Tension Forces in Suspended Bridges Using Time-Frequency Analysis

Gannon Stromquist-LeVoir, Kevin F. McMullen, Arash E. Zaghi, and Richard Christenson

Department of Civil and Environmental Engineering, University of Connecticut, Storrs, CT 06269, USA

Correspondence should be addressed to Kevin F. McMullen; kevin.mcmullen@uconn.edu

Received 30 August 2017; Revised 21 March 2018; Accepted 28 March 2018; Published 5 June 2018

Academic Editor: Michael Yam

A feasibility study was conducted to develop a novel method to determine the temporal changes of tensile forces in bridge suspender cables using time-frequency analysis of ambient vibration measurements. An analytical model of the suspender cables was developed to evaluate the power spectral density (PSD) function of a cable with consideration of cable flexural stiffness. Discrete-time, short-time Fourier transform (STFT) was utilized to analyze the recorded acceleration histories in both time and frequency domains. A mathematical convolution of the analytical PSD function and time-frequency data was completed to evaluate changes in cable tension force over time. The method was implemented using acceleration measurements collected from an in-service steel arch bridge with a suspended deck to calculate the temporal variation in cable forces from the vibration measurements. The observations served as proof of concept that the proposed method may be used for cable fatigue life calculations and bridge weigh-in-motion studies.

1. Introduction

The long-term viability of critical structural members is a major concern as our nation's infrastructure ages. Tension members of bridge systems such as suspender cables are susceptible to fatigue under vehicular traffic. Cyclical tensile loading of these members may lead to premature fatigue damage or failure [1]. The fatigue life of an element is dependent on the loading history. Traditionally, the fatigue life is determined using the stress-life method. *S-N* curves are empirically formulated to relate the nominal stress amplitude (S) and the number of cycles (N) until failure. The mean stress to which a particular member is subjected to is a combination of the oscillatory fatigue stress caused by transient loads and the permanent stress caused by dead loads. In order to accurately calculate the fatigue life of a member, equivalent stress amplitude must be calculated with respect to the mean stress using the relationship of either Goodman or Gerber [2]. A Haigh diagram is a graph of mean stress versus stress amplitude that may also be used to determine fatigue life (Figure 1) [3]. Several studies show that an increase in the mean stress may drastically reduce the estimated fatigue life of a member [4–6].

Since the mean stress has a substantial impact on the fatigue life of the member, it is critical to obtain an accurate history of the tension forces in fatigue-prone members such as cables. Suh and Chang conducted an experimental study on the fatigue behavior of wire ropes for hanger cables in suspension bridges and found that the mean stress on the cables had a significant effect on the fatigue performance of the cables [7]. The primary method that is conventionally used to monitor the tensile force variation in tension members is strain-based measurement by collecting strain data from strain gauges attached to individual members [8]. These data may be used to assess the stress and remaining fatigue life of structural members based on nominal stress amplitude [9]. If the strain gauges are applied to a member carrying permanent loads, then they can only determine the oscillatory stress amplitude, not the mean stress. Strain gauges must be applied prior to construction in order to capture the effects of dead load as well. Application of strain-based methods is also challenging because the strain gauges must be attached to the uneven surface of multistrand cables. Attaching strain gauges to uneven surfaces makes it difficult to achieve accurate readings. These are major shortcomings

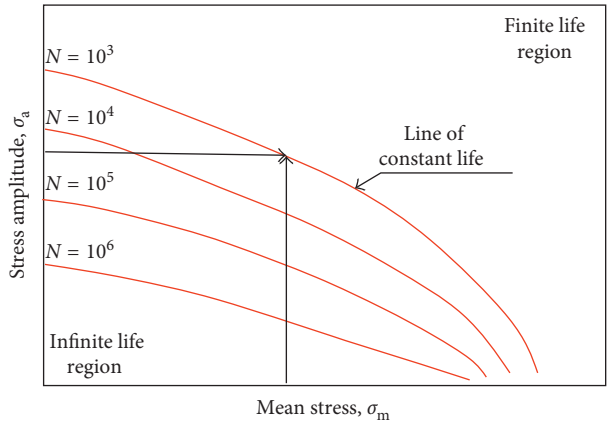

Figure 1: Example of a Haigh diagram for fatigue life estimation.

of strain-based fatigue analysis. Direct measurement may also be used to determine the tensile force in cables. However, this method is expensive and requires a load cell be integrated into the cable assembly in order to record the force supported by the cable.

Determining the mean tensile force in cables through vibration methods has been widely studied [10–12]. Frequency-based vibration methods may be simply, quickly, and accurately used to measure cable forces. The basic principle used in the formulation of vibration methods to determine tension forces from average frequency measurements is the taut string theory:

$$T = 4ml^2\left(\frac{f_n}{n}\right)^2, \quad (1)$$

where T is the tension force, m is the mass density, l is the length, n is the mode number, and f_n is the nth natural frequency. The frequency response of the cable may be captured by attaching accelerometers to individual cables to measure the vibration under loading.

However, this method may only be used to calculate mean tension force in the cables. Temporal changes in suspender cables under live load have a significant effect on the fatigue life of the member. According to NCHRP Report 538, there is no recognized standard to inspect or evaluate the in situ condition and strength of bridge cables [13]. Thus, a vibration-based method is needed to accurately determine the tension load history and remaining fatigue life of a cable. Vibration-based methods would reduce uncertainties associated with calculating the mean stress of a member because the total tension force on the cable directly influences the frequency of vibration of the cable. The total tension force consists of both dead load and moving load effects. Therefore, by monitoring the vibration of the cables, an accurate estimation of the axial tension force on the cables may be determined. By monitoring the vibration of the cable over a given window of time, the temporal changes in the cable force may be calculated. Understanding the variations in the tensile forces over time would facilitate estimation of the number of loading cycles and the extent of the fatigue damage on the cables. The time period of concern may be adjusted in terms of yearly, seasonal, monthly, daily, or hourly windows in order to capture long-term or short-term force changes in the cable. An additional advantage to a vibration-based method is that it would not require the application of strain gauges or the inclusion of load cells.

Several research projects have been conducted to evaluate the performance of cables used on suspension and cable-stayed bridges. Nakamura and Hosokawa [14] performed fatigue tests on parallel wire strand cables, which are typically used on cable-stayed bridges. It was noted that the fatigue life of the cables was dependent on their position on the bridge and the randomness of the traffic patterns requiring extensive analysis of the structure showing that load variation of individual cables affects its fatigue strength. Cunha et al. [15] conducted a dynamic test on the Vasco da Gama Bridge in Portugal by instrumenting several stay cables with accelerometers. An ambient vibration test and a free vibration test were performed to estimate the natural frequencies and mode shapes of each cable. The free vibration test was completed with a frequency domain multi-degree-of-freedom identification algorithm RFP (rational fraction polynomial) method when an impulse load was applied to the structure relating the vibration of the cable to the applied load; however, it was not directly related to the force in individual cables. Wong [16] monitored the structural condition of several bridges in Hong Kong including Tsing Ma, a suspension bridge, and Kap Shui Mun and Ting Kau, both cable-stayed bridges. The bridge health monitoring system (WASHMS) used for these projects estimated the forces in the stay cables based on the vibration amplitudes of the cables and the displacement of the cables under live load. Ren et al. [17] developed a set of empirical formulas to estimate the tension force in structural stay cables based on the fundamental frequency of the cable to determine mean force in the cables, but not temporal changes. Some other unique methods which have been used to measure in situ cable forces include Mehrabi's [18] proposed method to use laser-based vibration measurement of stay cables to determine cable force and Bao et al.'s [19] recommended new approach to calculate time-varying cable tension forces using adaptive sparse time-frequency analysis method.

The results presented in this paper are the results of a new methodology which was developed as a complementary part of an extensive research project aimed to evaluate the differences of cable tension forces in groups of cables through a series of stationary frequency analyses of cable acceleration data. In this complementary work, the feasibility of implementing a nonconventional, nonstationary frequency analysis was investigated. This paper presents the development and validation of this feasibility study and the formation of a new method to determine the fluctuation of tension forces in suspender cables over time with both adequate time and frequency resolution through acceleration measurements of the cable vibration. This study focuses on the application of nonstationary analysis on cable vibration data in time-frequency domain. The results of the stationary frequency analysis are presented in a detailed report by Stromquist-LeVoir et al. [20]. The nonstationary method proposed is intended to be a simple and easy-to-implement alternative approach to measure the time variation of cable tension due to

service loads. The intent of this paper is to demonstrate that time-frequency analysis can be used as an effective and practical approach to measure the time variation of suspender cable forces. Currently, frequency analysis is done mostly to measure baseline forces, not temporal changes.

2. Background and Methodology

The authors have developed a methodology which demonstrates the ability to relate temporal changes of the cable frequency to variations in axial tension force of the cable. The results show that the amplitude of the oscillatory tension force and corresponding fatigue stress in a suspender cable may be determined by relating vehicle traffic passing over the bridge to the vibration response of the cable. Developing a relationship between the in situ live load on a bridge and the tension in suspender cables has the potential to improve the current understanding of their short- and long-term performance under daily traffic. If the suspender cable forces are known under typical service conditions, then variation of the forces due to different environmental loads such as wind and thermal forces may be accounted for under extreme conditions. This allows the tensile force history in one or more cables to be directly related to the vibration frequency of the cable caused by the passing vehicles. This approach may be used to determine the remaining fatigue life of the member based on the long-term variation and cyclical loading of the cable tension forces.

Time-frequency analysis may be an effective and practical approach for engineers to estimate the remaining fatigue life in suspender cables. The unique load carrying mechanisms of bridges which use suspender cables prevent the use of traditional bridge monitoring techniques. A time history of cable acceleration may be used to measure the change in cable tension force induced by crossing vehicles. Therefore, a methodology may be developed to facilitate fatigue life analysis using a collection of cable acceleration time history data. The simplicity and accuracy of this proposed method would significantly benefit the engineering community.

Normally when accelerations are used in the majority of health monitoring applications, they only require knowing the frequency of the structure. However, to find the variance of tensile forces, the temporal variation of the vibration frequency is needed. Power spectrograms depict the change in frequency over time, but power spectral density (PSD) functions cannot show the time-varying nature of the signal. Thus, power spectrogram analysis was used to relate the acceleration time history data of the vibrating cable to the traffic load applied to the structure. The power spectrograms were determined using discrete-time short-time Fourier transform (STFT).

The discrete-time STFT described was used to analyze the acceleration data in time-frequency domain to identify the cable tension over time. The methodology does not require elaborate or intrusive instrumentation as does strain-based methods and direct measurement techniques. It also did not involve the development of an extensive model. An effective and efficient analytical dynamic model of the cable was developed and validated with experimental data. The novelty of this research lies in the development of averaging variations of the first few natural frequencies to achieve adequate resolution and accuracy in temporal analysis of suspender cables.

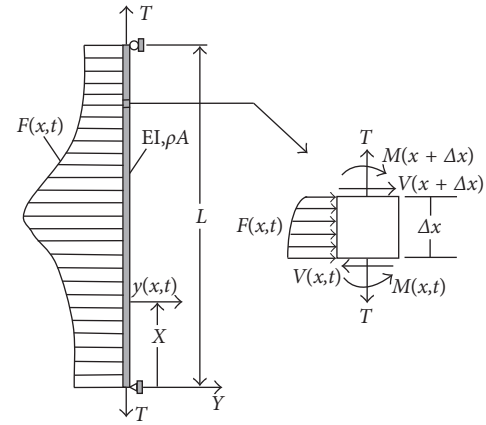

Figure 2: Analytic dynamic model of a suspender cable.

This method was used in a case study to evaluate variations in cable tension forces caused by vehicles passing over a bridge. Acceleration data were collected from suspender cables of a steel arch bridge with a suspended deck located in Connecticut to evaluate the applicability of the method for in-service bridges. The methodology and results presented in this study may be adapted and used to document tension force data for all applicable bridges in the National Bridge Index [21]. Studying the long-term performance of suspender cables will also allow the current fatigue load factors in the AASHTO LRFD to be refined [22].

3. Time Variations of Cable Tension Forces

The following sections outline the procedure for the proposed methodology. The time variation in cable tension forces was determined from acceleration time histories as follows: (1) the components needed to develop a representative analytical dynamic model of the cable system were identified; (2) each experimental acceleration data was transformed into a PSD function; and (3) the experimental PSD function was compared to the analytical model by varying the tension forces in the analytical model. The equations presented were used to estimate the cable tension force for a user-defined time period which could range from short term to long term depending on the frequency of data collection.

3.1. Analytical Dynamic Model Definition. An analytical model was developed to simulate the dynamics of a suspender cable. The system is composed of a single suspender cable with length, L, subjected to axial tension force, T, as shown in Figure 2 [23]. The model accounts for both geometric and bending stiffness. The mass and stiffness matrices were developed by subjecting the cable to an arbitrary time-varying transverse forcing function. The modal

vectors were orthogonal to both the mass and stiffness matrices for the rth mode, where r is any mode number. Since the stiffness of the flexible cable may be assumed to be relatively small, the boundary conditions for the model may be idealized as pin-roller since the cable stiffness will not generate significant moment fixity.

From the free body diagram, an infinitesimal section of cable at equilibrium has the following partial differential equation (PDE) of motion:

$$\rho A\ddot{y}(x,\ t) + \left[\mathrm{EI}y''(x,\ t)\right]'' - Ty''(x,\ t) = F(x,\ t), \quad (2)$$

where ρ is the material density, A is the cross-sectional area, $\ddot{y}(x,\ t)$ is the second derivative of deformation, that is, curvature with respect to time, EI is the bending stiffness of the cable, $y''(x,\ t)$ is the cable curvature with respect to the position along the longitudinal axis of the cable, T is the tension force in the cable, and $F(x,\ t)$ is an arbitrary transverse forcing function acting on the system (in Figure 2, $M(x,\ t) = EIy''(x,\ t)$).

Modal frequencies may be derived from the PDE of motion using modal coordinates. The modal mass and modal stiffness of the system for the rth mode may be found by (3) and (4), respectively:

$$M_r = \frac{\rho AL}{2}, \quad (3)$$

$$K_r = \frac{1}{2}\frac{\mathrm{EI}r^4\pi^4}{L^3} + \frac{1}{2}\frac{Tr^2\pi^2}{L}. \quad (4)$$

The natural frequency of the rth mode, ω_r, is calculated as

$$\omega_r = \sqrt{\frac{K_r}{M_r}} = \left(\frac{r\pi}{L}\right)^2\sqrt{\frac{\mathrm{EI}}{\rho A}} + \frac{r\pi}{L}\sqrt{\frac{T}{\rho A}}, \quad (5)$$

in radians per second. For a suspender cable pinned at both ends, the rth mode shape, $\varphi_r(x)$, at a given location, x, along the cable is a function of r half sine waves expressed as

$$\varphi_r(x) = \sin\left(\frac{r\pi x}{L}\right). \quad (6)$$

The modal damping for the system, C_r, is found as

$$C_r = 2M_r\omega_r\xi_r, \quad (7)$$

where ξ_r is the damping coefficient for the rth mode.

The mass, stiffness, and damping of the analytical model are used to develop state-space equations. The state-space equations are used to determine the frequency response function. The modal coordinate requires the deformed shape function, $y(x,\ t)$, to be represented by generalized modal displacements as shown by the following equation:

$$y(x,\ t) = \sum \varphi_r(x)q_r(t), \quad (8)$$

where $q_r(t)$ is the generalized modal displacement of the system. The equation of motion in the modal coordinates is given by the following equation:

$$M_r\ddot{q}(t) + C_r\dot{q}(t) + K_rq(t) = P_r(t), \quad (9)$$

where P_r is the modal force function given by:

$$P_r(t) = f(t)\alpha_r\frac{L}{2}, \quad (10)$$

where $f(t)$ is a single forcing function and α_r is the forcing function participation factor for the rth mode.

The state-space form may be rewritten to determine the frequency response function of the analytical model:

$$\begin{bmatrix}\dot{q}_r(t)\\ \ddot{q}_r(t)\end{bmatrix} = \begin{bmatrix}0_{rr} & \mathrm{Id}_{rr}\\ -M_r{}^{-1}K_r & -M_r{}^{-1}C_r\end{bmatrix}\begin{bmatrix}q_r(t)\\ \dot{q}_r(t)\end{bmatrix} + \begin{bmatrix}0_{rr}\\ \frac{\alpha_1 L}{2M_1} & 0\\ & \ddots\\ 0 & \frac{\alpha_r L}{2M_r}\end{bmatrix} f(t), \quad (11)$$

where 0_{rr} is a matrix of zeros with r rows by r columns and Id_{rr} is the identity matrix of with r rows by r columns. The output equation, $y(x,\ t)$, for the system is determined using the decoupling equation used to determine the modal system shown in (8):

$$y(x_{\mathrm{out}}) = \begin{bmatrix}\varphi_r(x_{\mathrm{out}})_{1xr} & 0_{1xr}\end{bmatrix}\begin{bmatrix}q_r\\ \dot{q}_r\end{bmatrix} + 0_{1x1}f(t), \quad (12)$$

where x_{out} is the location at which the response of the cable is needed. These state-space equations are used to determine the frequency response functions at a given location along the length. This in turn may be used to compute the PSD function.

Equations (11) and (12) are used to obtain the input-to-output transfer function of the system in the frequency domain. This is achieved by taking the Laplace transform of both equations and rearranging (11) to substitute it into the Laplace transform of (12). Finally, the ratio of Laplace output, $Y_r(s)$, to the Laplace input, $U_r(s)$, represents the transfer function, TF or $H_r(\omega)$, of the system. Using the relationship between Laplace transformation and natural frequency, $s = i\omega$, the transfer function may be defined by the following equation:

$$H_r(\omega) = \frac{Y_r(\omega)}{U_r(\omega)}, \quad (13)$$

where $Y_r(\omega)$ and $U_r(\omega)$ are the Fourier transform of the output and input, respectively.

Bode plots were used to compare the magnitude of the system's response in dB to the frequencies of the cable vibration under loading. A bode plot provides a powerful visualization for system responses in the frequency domain. The bode plot includes r magnitude and r phase functions for each input force. The total TF of the system is obtained by superimposing the individual TFs in order to determine the

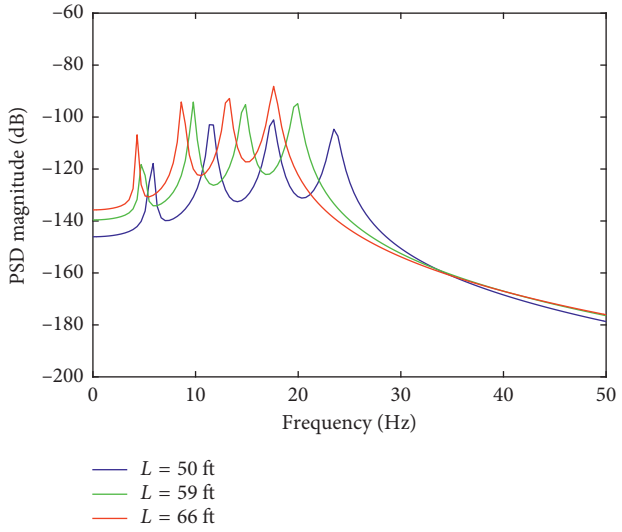

Figure 3: Analytic PSD function length comparison.

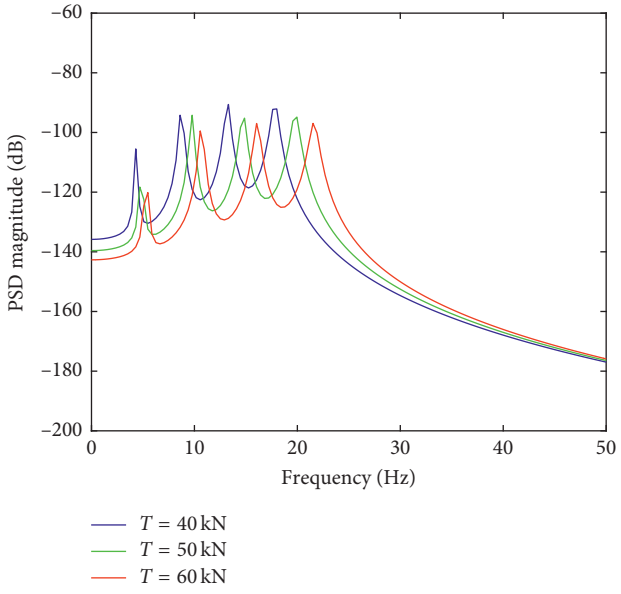

Figure 4: Analytic PSD function tension force comparison.

overall system response. The end goal of the analysis was to generate the PSD function plot of the system under an ideal white noise input. The white noise input was an assumption made to obtain the PSD function plot from the TF of the state-space equations. Under ideal white noise, all frequencies within the band of interest are equally excited and the input Fourier transform magnitude is equivalent at all frequencies. If the white noise assumption is upheld, (13) simplifies to show that the TF is equivalent to the Laplace transform of the output, $H_r(\omega) = Y_r(\omega)$.

The following definition allows a Fourier transform to be modified into a PSD function by the subsequent process. The PSD function is defined as the square of the Fourier transform series divided by its length:

$$G_r(\omega) = \left(\frac{|H_r(\omega)|}{\text{length}\left(|H_r(\omega)|\right)} \right)^2, \tag{14}$$

where $G_r(\omega)$ is the PSD function of transfer function, $H_r(\omega)$. The analytical PSD function was compared to the experimental PSD function determined from acceleration values to validate the analytical dynamic model of the cable. Further explanation is provided in the following section.

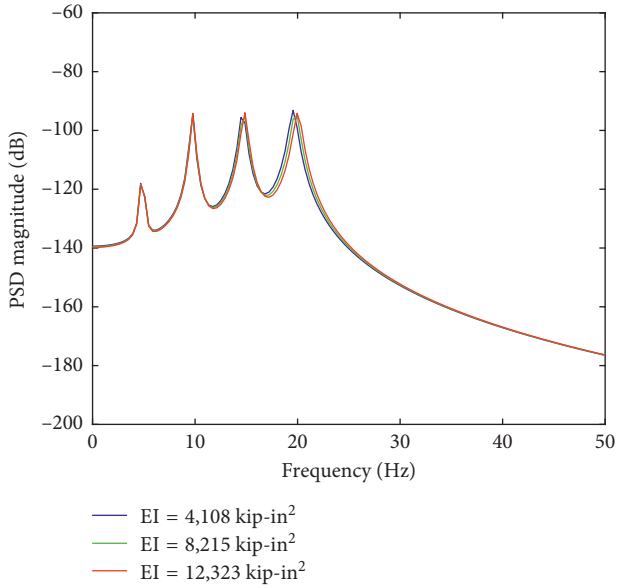

Figure 5: Analytic PSD function cable stiffness comparison.

3.2. Effect of Cable Length, Tension, Stiffness, and Damping on PSD Function. To understand the effect of certain significant cable parameters on the PSD function of the analytical model, a parametric study was performed. The parameters considered were cable length, tension force, cable bending stiffness, and damping ratio. Only one parameter was varied for each mode to show the effect of that parameter on the first four fundamental frequencies of the analytical system. Figures 3–6 illustrate the changes in the fundamental frequency for each of the parameters tested in the parametric study. Figure 3 depicts the PSD functions for three cable lengths that varied from 15.24 m to 20.12 m (50 ft to 66 ft). Figure 4 depicts the PSD functions for a 15.24 m (50 ft) cable subjected to three tension forces varying from 178 kN to 267 kN (40 kip to 60 kip). Figure 5 depicts the PSD functions for a 15.24 m (50 ft) cable with a 222 kN (50 kip) tension force with three cable bending stiffness values varying from 11.8 kN-m^2 to 35.4 kN-m^2 (4,108 kip-in.^{2} to 12,323 kip-in.^{2}). Lastly, Figure 6 depicts the PSD functions for a 15.24 m (50 ft) cable with 222 kN (50 kip) tension force, a cable bending stiffness of 23.6 kN-m^2 (8,215 kip-in.^{2}), and three damping ratios varying from 1% to 5%. The results presented in Figures 3–6 were in agreement with the relationship presented in (5). Figures 3 and 4 are evidence that changing the cable length or tension force has a significant impact on the first four natural frequencies of the system. Figure 5 shows that changing the bending stiffness does not significantly change the natural frequency. However, changing the

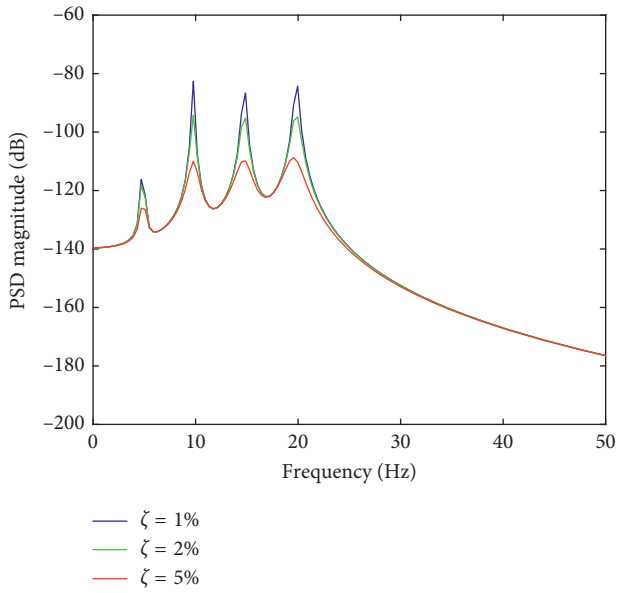

Figure 6: Analytic PSD function damping ratio comparison.

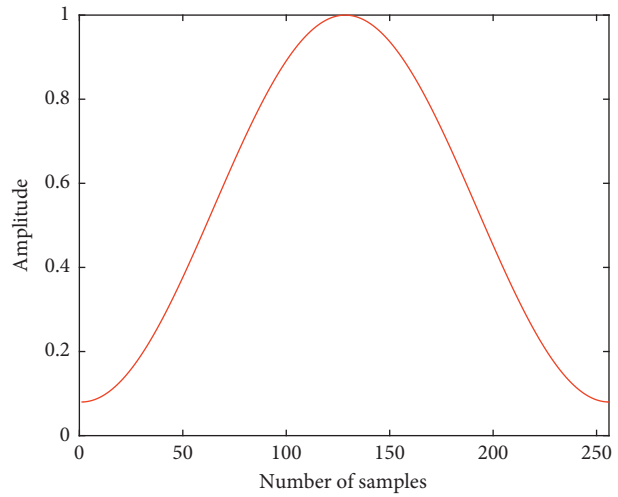

Figure 7: Hamming window.

damping ratio does not change the value of the natural frequencies significantly but changes the amplitude of each peak as shown in Figure 6. Therefore, it may be conclude that variations in cable lengths and cable tensions have a significant effect on the results of the PSD function, whereas the damping ratio only affects the magnitude of the response and the cable stiffness has relatively no effect. A full sensitivity analysis may be conducted in order to categorize the significance of each parameter on the PSD function results.

3.3. Experimental Power Spectral Density. This section outlines the method for generating a PSD function from field data. On a suspension-type bridge, the tension forces in cables change due to varying excitation from traffic loading. Because the tension force in a particular cable changes as the vehicle passes, a frequency domain analysis will show the dominant frequencies of vibration. STFTs were used to obtain valuable information from a smaller window of data to show the time-varying vibration characteristics. These STFTs showed changes in the natural frequencies of the cable over time and consequently the corresponding variations in cable tension.

For a given acceleration time history, $\ddot{x}(t)$, a discrete Fourier transform (DFT) was used to transform time domain data to the frequency domain as shown by the following equation:

$$\ddot{X}(\omega) = \sum_{n=0}^{N-1} \ddot{x}(n) e^{-j\omega n \Delta t}, \tag{15}$$

where $\ddot{X}(\omega)$ is the acceleration time history transformed into the frequency domain, N is the total number of values in the sequence, $j = \sqrt{-1}$, and Δt is the time step. Temporal resolution of the frequency content was required to observe changes in frequency content over time and to fully understand the short-term behavior of a given signal. The time-frequency transformation was conducted using the discrete-time STFT algorithm. While the original Fourier transformation was applied on the entire data set as indicated in (15), a STFT sectioned the data set into small windows which were then analyzed by the DFT. Sectioning of the data was completed using a Hamming window. The Hamming window function is a smooth and bell-shaped curve as shown in Figure 7. The data were isolated into individual intervals to allow for filtering of the data. All values outside were taken as zero in order to reduce the side lobes created from the Fourier transformation. The window segments were moved and repeated for each time interval allowing for overlap to increase the temporal resolution without sacrificing frequency resolution. The mathematical representation for the STFT is given by the following equation:

$$\ddot{X}(\omega,\ p) = \sum_{p=1}^{N_w} \sum_{n=0}^{N-1} \left(\ddot{x}(n) w_{pn}\right) e^{-j\omega n \Delta t}, \tag{16}$$

where $\ddot{X}(\omega,\ p)$ is the acceleration signal in the frequency domain, p is the window number, N_w is the total number of windows, N is the number of points used in the Fourier transform, and w_{pn} is the value for the window at a given window segment and data point. The value for w_{pn} was selected to be a Hamming window as described by the following equation:

$$w_{pn} = 0.54 - 0.46 \cos\left(\frac{2\pi n}{N-1}\right). \tag{17}$$

Equation (16) was used to perform Fourier transformations on many segmented data sets. The process of generating a PSD function from the STFT is identical to the process for generating the PSD function from the analytical model. That is, the PSD function is the square of the Fourier transform series divided by its length as shown by the following equation:

$$P_{xx}(\omega,\ p) = \left(\frac{|\ddot{X}(\omega,\ p)|}{N}\right)^2, \tag{18}$$

where $P_{xx}(\omega,\ p)$ is the PSD function of the experimental data. This function was graphed over the range of frequencies

Table 1: Cable lengths.

Cable set	L2/L18	L3/L17	L4/L16	L5/L15	L6/L14	L7/L13	L8/L13	L9/L11	L10
Length (m)	3.4	7.9	11.9	15.2	18.0	20.1	21.6	22.6	22.9

in order to indicate the natural frequencies for each experimental data set for a user-defined time window. These time windows must be optimized in order to balance both time and frequency resolution. A longer time window will capture global changes while a shorter time window will capture local changes, for example, changes due to live load traffic.

4. Obtaining Temporal Cable Tension Forces (Beta Algorithm)

The tension force time history was determined by evaluating the temporal changes of frequency content of a cable because the frequency response of a dynamic cable system varies with respect to the tension force in the cable. The time resolution of the PSD function from (18) had to be fine enough to track the temporal changes of the tensile force. Thus, the recorded acceleration history was split into multiple window segments. This required an automated approach to detect and quantify the temporal changes in tension forces. The experimental tension forces were determined by finding the convolution of the experimental and analytical PSD functions. A convolution is a mathematical operation on two equations producing a third that gives the area of overlap between the two equations as a function of the translational shift of one of the original equations. The translation was performed by changing the window number, p, in (16). The convolution function in this study, β, is evaluated by the following integral:

$$\beta(p) = P_{xx}(\omega,\ p) * G_{xx}(\omega) = \int_0^{\pi f_s} P_{xx}(\omega,\ p) \cdot G_{xx}(\omega) d\omega, \tag{19}$$

where f_s is the sampling frequency in hertz. A range of tension forces was considered to create an array of β values because the analytic PSD function, $G_{xx}(\omega)$, is a simple function of the cable tension force as presented in (14). However, the convolution integral of (19) was estimated through numerical summation rather than integration. The assumed value of cable tension force that resulted in the maximum value for $\beta(p)$, $\beta_{\max}$, defined the cable tension force for the specific window. This process was repeated for all window segments to determine the change in cable tension force over the total time range covered by the window segments. The stepwise algorithm used to obtain the time variation of tension force in a cable is as follows:

(1) The PSD function of the collected acceleration data was obtained, and the fundamental frequency was found.

(2) Equation (5) was used to find the mean cable tensile force, T_{mean}.

(3) A range for cable tension forces was assumed based on loads imposed by the weight and axle configuration for a crossing vehicle with a central value of T_{mean}. The assumptions vary depending on the type and geometry of the bridge.

(4) Using the analytical model, the analytical PSD function was calculated for each tension force at the location where the experimental measurements were collected.

(5) The time-frequency domain transformation of the measured data was obtained using STFT.

(6) For each analytical PSD function obtained in Step 4, the convolution with the experimental PSD function of the pth window, $\beta(p)$, was found.

(7) For each time window, the tensile force that corresponds with value $\beta_{\max}$ was found.

(8) A plot for the tensile force of Step 7 versus the time representing the pth time window was created to obtain the tensile force history.

In practice, Steps 1–4 may be precalculated and Steps 5–8 may be computed as the data is collected. The tensile force history may be used to gain a better understanding of the in situ fatigue life of the cables by accurately determining the true number and magnitude of the stress range in the cables. These potential applications will be further discussed in a case study of the Arrigoni Bridge in the following section.

5. Case Study: The Arrigoni Bridge

A case study of the Arrigoni Bridge was used to demonstrate the proposed methodology for obtaining time variations of the tension force in suspender cables. The Arrigoni Bridge was selected because it is a steel arch bridge with suspender cables attached to the bridge deck and a predictable force distribution in the suspender cables. The experimental results collected from this bridge were compared with the analytical model to verify the proposed methodology.

5.1. Arrigoni Bridge. The Arrigoni Bridge is a through arch bridge with a cable suspended deck connecting the towns of Middletown and Portland, Connecticut. The bridge crosses the Connecticut River and was opened to traffic in 1938. The two main spans are each 183 m (600 ft). The bridge deck is a composite girder system supported by sets of four vertical, helical suspender cables which connect the deck to the trusses. The cables vary in length from 3.35 m to 22.86 m (11 ft to 75 ft). The full breakdown of all the cable sets is provided in Table 1. The Arrigoni Bridge has a daily traffic volume of 33,600 vehicles. It is the only river crossing for more than 16.1 km (10 miles) in either direction, making it a critical link in the local transportation network. A picture of the bridge and its suspender cables is shown in Figure 8.

The two spans of the bridge are similar. Therefore, data were only collected from cables on one of the spans and because of symmetry these data may be accurately extended to represent the other span.

Figure 8: Arrigoni Bridge.

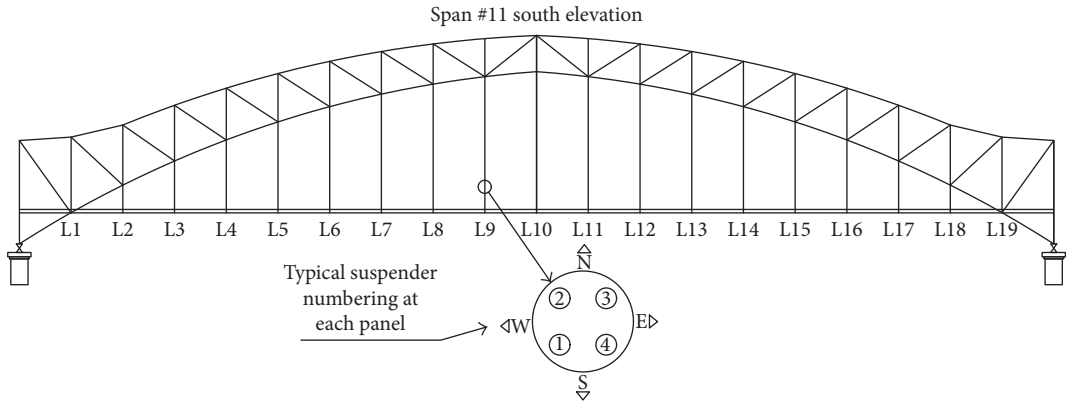

Figure 9: Suspender cable layout.

5.2. Suspender Cable Parameters. The numbering system used to identify the cables was aligned with the vertical members of the steel truss, labeled L2 through L18. Within each set, the individual cables were labeled 1–4, starting in the SW corner and continuing clockwise. The numbering convention is shown in Figure 8.

Cable sets are spaced at 9.14 m (30 ft). The length of each cable was determined from design plans provided by the Connecticut Department of Transportation and verified with field measurements. The length of the four cables in each cable set was assumed to be equal.

The Arrigoni Bridge suspender cables were examined using magnetic flux, nondestructive testing to determine their overall condition and identify abnormalities such as broken or loose strands [24]. The magnetic flux method determines the condition of the cable by recording the magnetic field of a magnetized cable. The suspender cables were assumed to have their full cross-sectional area based on the results of the investigation. The nominal diameter and cross-sectional area of the cables were 41.275 mm (1.625 in) and 1,026 mm^2 (1.59 in^2), respectively. A diagram of the cross-section of the cables is shown in Figure 9.

The mass per unit length of the cables was determined by multiplying the cable material density by the cross-sectional area. The cables were assumed to have been made of standard structural steel with a density of 77 kN/m^3 (490 lb/ft^3). This resulted in a weight per unit length of 79 N/m (5.41 lb/ft) and a mass per unit length of 8.04 g/m (0.168 lb-s^2/ft^2). As stated in ASTM A586, the minimum Young's modulus of the cables is 164.5 kN/mm^2 (24,000 ksi).

5.3. Sensors and Data Acquisition. A Bridge Diagnostics Incorporated (BDI) Structural Testing System with wireless data acquisition (STS-WiFi) was used to collect the cable acceleration histories. The system was comprised a base station, three nodes, twelve BDI 50 g accelerometers where g refers to the acceleration due to gravity, and a laptop PC. Four accelerometers and one of the nodes are shown in Figure 10. The STS-WiFi base station aggregates the data and transmits it wirelessly to the PC where the data may be viewed and stored. The accelerometers were oriented to capture vibration of the cables along the longitudinal axis of the bridge, that is, the horizontal axis of the cables. They were positioned parallel to the roadway and attached to the cover of the suspender cables with Velcro straps. The sensors were placed 1.52 m (5 ft) above the bridge deck, 2.9 m (9.5 ft) above the bottom anchor of the cables. This yielded an x/L value of 0.19 for a 15.24 m (50 ft) cable. The sensors were located at this height for ease of access and to keep all lanes on the bridge open to traffic during testing. The cable excitation at this location had sufficient vibration energy to determine the natural frequencies of the cables. While the locations of the accelerometers for this case study were not optimized based on the vibrational mode shapes, it was possible to accurately calculate the tension forces confirming the applicability of the methodology.

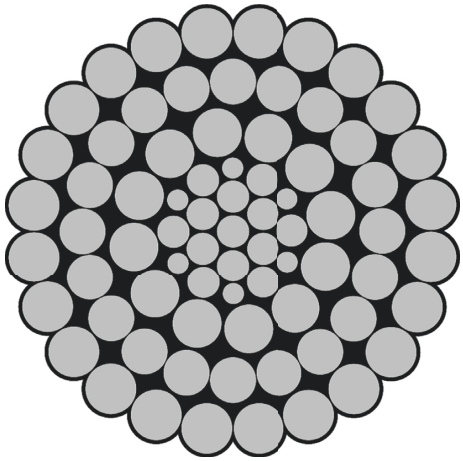

Figure 10: Cross section of the individual suspender cables.

Figure 11: Four accelerometers of the STS-WiFi system used on Arrigoni Bridge.

Data were collected at a sampling rate of 100 Hz under normal ambient vibration induced by traffic and typical wind. Data collection did not depend on the type of traffic, excitation, and so on The method proved to be capable of generating reliable results even in cases with high noise-to-signal ratios because of the type of sampling used and the nonstationary windowing implemented. A subset of the data for cables L5, L6, and L7 on the south side of the Arrigoni Bridge was considered in the present analysis and discussion. The acceleration data for these cables were collected simultaneously. These cables represented a large variety of distinct vibration modes in a spectrogram analysis of the time history data. Figure 11 shows the acceleration histories of individual cables in each cable set.

Table 2: Time and force resolution for different window sizes.

Window size (number of points)	Number of Fourier transform points	Time resolution (sec)	Force resolution (kN)
64	64	0.06	6.98
128	128	0.13	3.47
256	**256**	**0.26**	**1.73**
512	512	0.51	0.85

Table 3: Alpha values for each cable set.

Cable set	α_1	α_2	α_3	α_4
L5	0.05	0.25	0.50	1.00
L6	0.10	0.25	0.30	0.50
L7	0.05	0.25	0.50	0.75

Effective transformation of the acceleration data into the time-frequency domain greatly influences the efficiency of the procedure. MATLAB v7.10.0 [25] was used to perform the mathematical calculations. To maximize efficiency, several transformation parameters were studied to determine which combination produced the most functional time-frequency data. These parameters include the size and overlap of the window and the number of fast Fourier transform (FFT) points. Based on the study of these parameters, the STFTs were generated using a Hamming window size of 256 data points with a 90% window overlap. The 90% window overlap was selected over a standard 50% overlap to increase the temporal resolution of the spectrogram by creating more windowed segments. The frequency limit was set for usable results in order to balance the resolution of both the time of data collection and the tension force. In time-frequency analysis, there is a tradeoff between accuracy of the data and resolution of the data. Since frequency resolution of the cables is critical in determining tensile forces in the cables, a larger window overlap was chosen. Table 2 presents the different parameters that were examined along with their time and force resolution. A time resolution of 0.26 seconds and a force resolution of 1.7 kN (0.39 kip) were found to be optimal for this study.

Only the first four modes of vibration were considered in the analytical model for this case study. It was observed that higher modes of vibrations were not clearly depicted on the FFT curves due to the signal-to-noise ratio of the acceleration data collected at higher frequencies. A 3% damping was used for each mode. This damping value was chosen for the analytical model to ensure that the frequency of each mode of cable vibration was captured since adjusting the damping for the cable shifts the frequency of each mode. A damping ratio of 3% was chosen because of its strong agreement with the experimental results of the modal frequency of the cables. The modal frequency of the models was found to be the critical value for determining the force in the cables. Other damping ratios were investigated, but did not capture the modal frequencies found from the field measurements.

5.4. Results of the Case Study. The force time history results for all of the cables except for cables L5-1 and L5-2 are

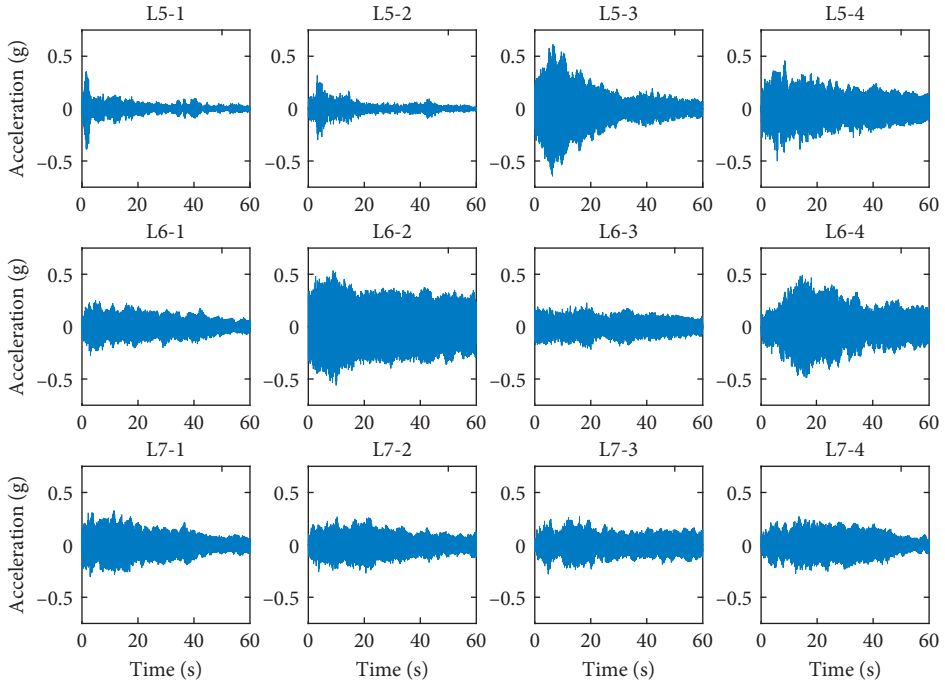

Figure 12: Acceleration time histories.

presented in this section. None of the modes of cables L5-1 and L5-2 had strong magnitude values to accurately use for the PSD analysis. The magnitude values were low for the PSD analysis when the energy between the natural frequencies was too great or the excitation was too low. If the amount of noise between the modal frequencies was too large, it made it impossible to identify distinct peaks in the data. The natural frequency of the cable must be identified to accurately determine the tension force of the cable. Therefore, the tension force changes in cables L5-1 and L5-2 could not be measured.

Initially, the forcing function participation factors were determined by comparing the experimental and analytical PSD functions. Table 3 presents the α_r values for each of the modes in this system. Figure 12 compares the experimental and analytic PSD functions for cable L5-3. The steep drop-off of the analytic PSD function after the fourth mode was the result of only including the first four modes in the analysis.

The range of tensile forces was selected based on the approximate T_{mean} as described in Step 3 of the methodology. This range was also used to determine the effective range of β. The value for the fundamental frequency was determined by visual inspection of the frequency analysis, which was used to determine T_{mean}. The range of candidate tensile forces in this case study is defined as follows:

$$0.9T_{\text{mean}} \le T \le 1.1T_{\text{mean}}, \tag{20}$$

where T is the set of candidate cable tension forces for the analytical PSD function. The coefficients 0.9 and 1.1 were determined because the variation of cable tension was no more than 6% for all cases studied. These bounds do not constrain the algorithm and capture a change of ±10% in the cable tension. The convolution of experimental and analytical PSD functions was evaluated for T_s at an interval of 0.001 T_{mean} to ensure that $\beta_{\max}$ was captured with sufficient accuracy.

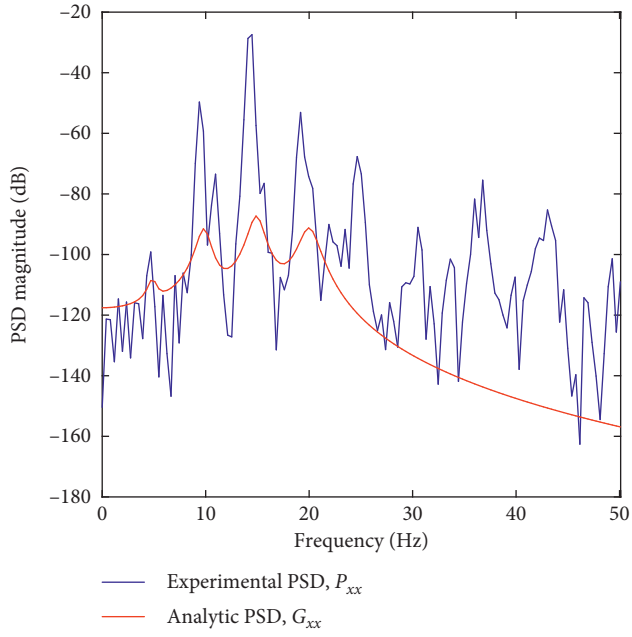

Figure 13: Comparison between analytical and experimental PSD functions.

5.5. Estimating Cable Tension Force History. The cable tension force histories obtained using the proposed algorithm are presented in Figure 13. The mean cable tension force for all cables in the three cable sets ranged from 156 kN to

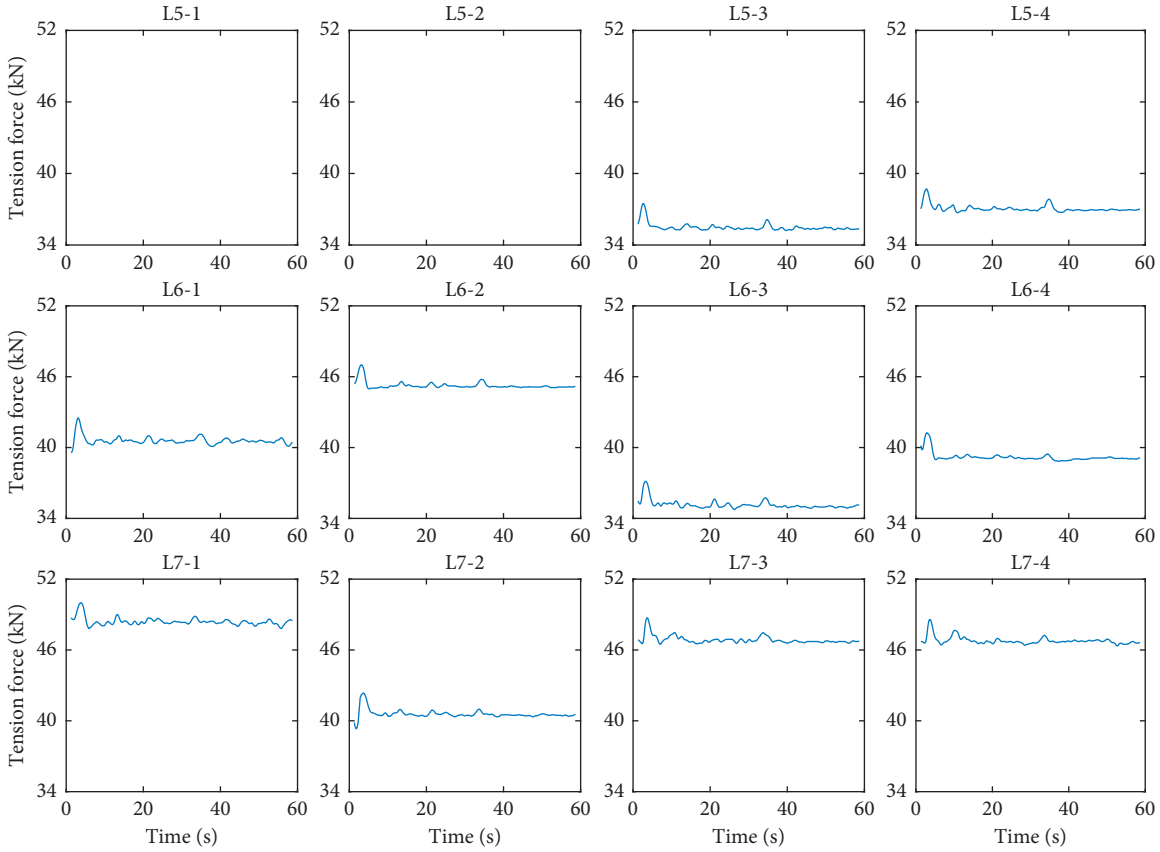

Figure 14: Cable tension force histories.

227 kN (35 to 51 kips). The tension force in individual suspender cables varied due to the fluctuation of live load demand on each cable [26]. Figure 14 shows the time history for each cable with vibration oscillation around the individual cables mean tension force. All of the graphs presented in Figure 14 show a peak at approximately three seconds. The consistent increase was due to a truck crossing the bridge at this time. During the peak loading, the force in the two cables in cable set 5 increased by approximately 5% due to the live load introduced by the truck. The force in cable set 6 increased by 4–6% and in cable set 7 by 4-5%.

A close-up view of the cable tension force histories is shown in Figure 15. The figure illustrates that the shape of the event was similar for cables in the same set, but the increase in tension force varies between individual cables. The values of the peak force change and the maximum total change within each set are presented in Table 4. The maximum total change in tension force was found after adding all of the force histories of each cable within a cable set. Because the values for two of the four cables in set L5 were not present, the maximum total change was obtained by doubling the values of the two cables that were measured.

The consistent values presented in Table 4 are evidence that the amplitude of the tension force caused by the crossing vehicle was approximately 33.4 kN (7.5 kips). In the current test setup, the weights of the vehicles crossing the bridge are unknown. The tension force amplitude is not expected to be the same as the weight of the vehicle due to the force distribution between structural members. However, the peak tension force may be used to predict the stress amplitude in the individual cables.

The speed of the vehicle may also be estimated from the results presented by calculating the time lag between the peak moving load impacts on each of the suspender cable sets since the cables are spaced at equal spacing. The spacing between the cables is 9.14 m (30 ft) which corresponds to the distance which the vehicle traveled. By dividing the spacing between the cables by the time between the peak forces in each cable, the speed of the vehicle may be calculated. Since the peaks in the cable sets in Figure 16 are spaced approximately 0.5 seconds apart for the maximum forces in cable sets L5, L6, and L7, the speed of the vehicle is approximately 64 km/hr (40 mph), which is close to the posted speed of 56 km/hr (35 mph). In addition, Figure 15 shows that the peak forces in the individual cables within the cable sets occur simultaneously, which indicates that the differences in the peak force between cable sets are due to external live load effects.

This method not only gives the amplitude of tension forces in the individual cables, but also provides the mean tension force that was present from the permanent loads on the structure. The mean tension force coupled with actual temporal variation in cable forces is invaluable for evaluating fatigue life. Using these methods would allow authorities to capture a more accurate picture of the cable stress history and inform bridge owners of the remaining fatigue life of the suspender cables.

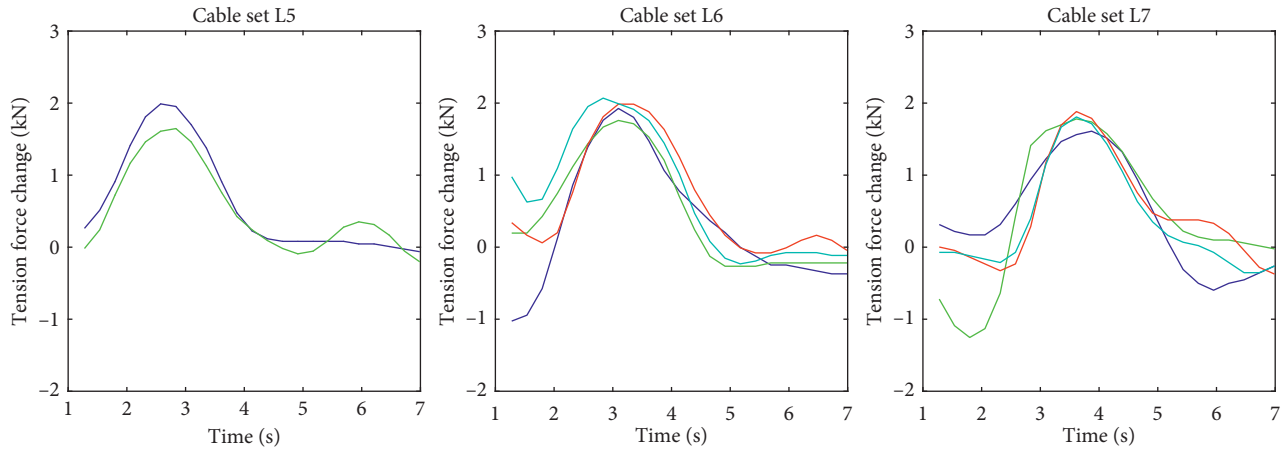

Figure 15: Time history of variation of tensile forces of individual cables in each set.

Table 4: Peak force (kN) change results.

Cable set	Cable number				Average of the peak change (kN)	Maximum total change (kN)
	1	2	3	4		
L5	—	—	9.061	7.442	8.251	33.006
L6	7.024	5.978	9.524	9.759	8.074	32.294
L7	9.141	8.963	9.648	8.020	8.945	35.781

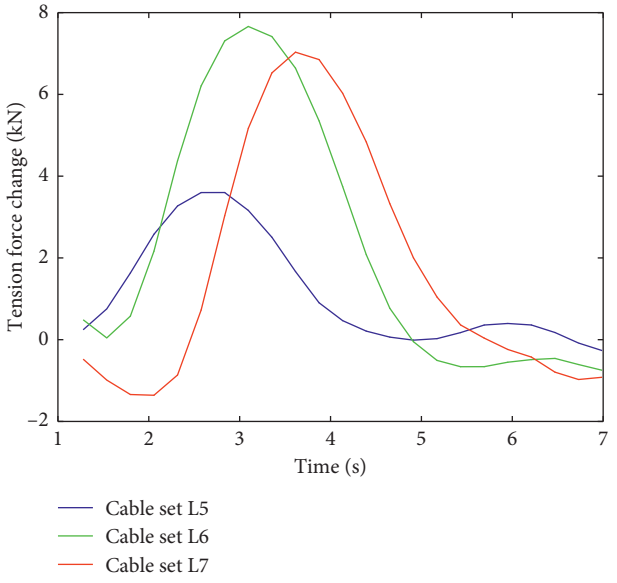

Figure 16: Time history of variation of the total forces in each cable set.

6. Summary and Conclusions

In this study, a novel method is presented to estimate temporal variation of cable tension forces. An analytic model subjected to an arbitrary, time-varying, transverse forcing function was used to develop a system of state-space equations. The model accounted for both cable tension force and bending stiffness. These equations were used to evaluate the power spectral density (PSD) functions of the analytical model. Likewise, a PSD function was developed based on a short-time Fourier transform (STFT) of experimentally measured accelerations of a bridge suspender cable. The cable tension force was determined by identifying the analytical force that maximized the result of the convolution of the two PSD functions found using the beta algorithm equation. This process identified not only the temporal variation of cable tension, but also the baseline cable tension using the recorded suspender accelerations. Including the baseline tension force was critical when examining the fatigue stress of the cable.

To determine the robustness and applicability of the proposed method, a case study was performed. Experimental data were collected from the Arrigoni Bridge located between Middletown and Portland, Connecticut. Results from this case study showed the method had the ability to measure the fluctuation of tension forces caused by a passing vehicle. The measured change in suspender tension force due to an unknown passing truck was estimated as 33.4 kN (7.5 kips). The results of this case study are evidence that the presented method may be used to determine the existing baseline cable tension as well as measuring variations in cable tension due to traffic.

7. Future Work

Further research is required in order improve upon the methodology presented in this paper. Experimental tests should be conducted using direct for measuring techniques in order to quantify the accuracy of the proposed method. A full probabilistic analysis should also be completed to determine the effects of each parameter on the results, so that the uncertainties in the results may be accurately identified. The results presented in this paper demonstrate that

time-frequency analysis may be used as an effective and practical approach to measure the time variation of suspender cable forces. Adapting this methodology may allow engineers to better estimate the remaining fatigue life of suspender cables by calculating the variation in tensile force based on its relationship to the frequency of vibration. This method may also adopted for use for bridge weight-in-motion (BWIM) studies if a complete analytical model of the structure is developed and calibrated by loading the bridge with a truck of known weight. The procedure presented may be applicable to any bridge type which includes cables due to the basic theory of the relationship between force and frequency of vibration. However, attention should be taken when applying the method to tension rods as opposed to cables due to the added flexural stiffness.

Conflicts of Interest

The authors declare that they have no conflicts of interest.

Acknowledgments

The authors gratefully acknowledge the support of this research by the Connecticut Department of Transportation and the U.S. Federal Highway Administration. The authors would like to thank the Connecticut Transportation Institute and the in Connecticut Department of Transportation for their help in collecting the data used in this paper. The student support of Dr. Kevin Zmetra, Dr. Alicia Echevarria, and Alexandra Hain is also thanked.

References

[1] J. A. Bannantine, J. J. Comer, and J. L. Handrock, *Fundamentals of Metal Fatigue Analysis*, Prentice Hall, Upper Saddle River, NJ, USA, 1990.

[2] T. Nicholas, *High Cycle Fatigue: A Mechanics of Materials Prospective*, Elsevier Science, New York, NY, USA, 2006.

[3] D. Maxwell and T. Nicholas, "A rapid method for generation of a Haigh diagram for high cycle fatigue," in *Fatigue and Fracture Mechanics: 29th Volume*, ASTM, West Conshohocken, PA, USA, 1999.

[4] Q. Bader and E. Kadum, "Mean stress correction effects on the fatigue life behavior of steel alloys by using stress life approach theories," *International Journal of Engineering and Technology*, vol. 14, no. 4, 2014.

[5] N. E. Dowling, C. A. Calhoun, and A. Arcari, "Mean stress effects in stress-life fatigue and the Walker equation," *Fatigue and Fracture of Engineering Materials and Structures*, vol. 32, no. 3, pp. 163–179, 2009.

[6] J. Schijve, "Fatigue of structures and materials in the 20th century and the state of the art," *International Journal of Fatigue*, vol. 25, no. 8, pp. 679–702, 2003.

[7] J. I. Suh and S. P. Chang, "Experimental study on fatigue behaviour of wire ropes," *International Journal of Fatigue*, vol. 22, no. 4, pp. 337–347, 2000.

[8] Y. Zhou, "Assessment of bridge remaining fatigue life through field strain measurement," *Journal of Bridge Engineering*, vol. 11, no. 6, pp. 737–744, 2006.

[9] J. R. Casas, "A combined method for measuring cable forces: the cable-stayed Alamillo bridge, Spain," *Structural Engineering International*, vol. 4, no. 4, pp. 235–240, 1994.

[10] Z. Fang and J. Q. Wang, "Practical formula for cable tension estimation by vibration method," *Journal of Bridge Engineering*, vol. 17, no. 1, pp. 161–164, 2010.

[11] H. Max Irvine, *Cable Structures*, MIT Press, Cambridge, MA, USA, 1981.

[12] G. Nugroho, H. Priyosulistyo, and B. Suhendro, "Evaluation of tension force using vibration technique related to string and beam theory to ratio of moment of inertia to span," *Procedia Engineering*, vol. 95, pp. 225–231, 2014.

[13] R. M. Mayrbaurl and S. Camo, *Guidelines for Inspection and Strength Evaluation of Suspension Bridge Parallel Wire Cables*, NCHRP Report 534, Weidlinger Associates Inc., New York, NY, USA, 2004.

[14] S. Nakamura and H. Hosokawa, "A study on the fatigue design of parallel wire strands on cable-stayed bridges," *Structural Engineering/Earthquake Engineering*, vol. 6, no. 2, 1989.

[15] A. Cunha, E. Caetano, and R. Delgado, "Dynamic tests on large cable-stayed bridge," *Journal of Bridge Engineering*, vol. 6, no. 1, 2001.

[16] K. Y. Wong, "Instrumentation and health monitoring of cable-supported bridges," *Structural Control and Health Monitoring*, vol. 11, no. 2, pp. 91–124, 2004.

[17] W. Ren, G. Chen, and W. Hu, "Empirical formulas to estimate cable tension by cable fundamental frequency," *Structural Engineering and Mechanics*, vol. 20, no. 3, pp. 363–380, 2005.

[18] A. Mehrabi, "In-service evaluation of cable-stayed bridges, overview of available methods and findings," *Journal of Bridge Engineering*, vol. 11, no. 6, pp. 716–724, 2006.

[19] Y. Bao, Z. Shi, J. L. Beck, H. Li, and T. Y. Hou, "Identification of time-varying cable tension forces based on adaptive sparse time-frequency analysis of cable vibrations," *Structural Control and Health Monitoring*, vol. 24, no. 3, p. e1889, 2017.

[20] G. Stromquist-LeVoir, R. Christenson, J. DeWolf, and J. Kim, *Validating and Assessing Integrity of Troubled Bridges in Connecticut: Monitoring Cable Tensions for the Arrigoni Bridge, Middletown, CT*, Report No. CT-2270-F-13 -11, Connecticut Department of Transportation, Newington, CT, USA, 2013.

[21] Federal Highway Administration (FHWA), *National Bridge Inventory*, 2005, https://www.fhwa.dot.gov/bridge/nbi.cfm.

[22] American Association of State Highway and Transportation Officials (AASHTO), *LRFD Bridge Design Specifications*, AASHTO, Washington, DC, USA, 7th edition, 2015.

[23] J. W. Tedesco, W. G. McDougal, and C. A. Ross, *Structural Dynamics: Theory and Applications*, Addison Wesley, Menlo Park, CA, USA, 1999.

[24] R. Martyna, *Record of Electromagnetic Examination of Suspender Cables*, Connecticut Department of Transportation, Newington, CT, USA, 2007.

[25] The MathWorks Inc., *MATLAB Version 7.10.0*, The MathWorks Inc., Natick, MA, USA, 2010.

[26] Y. An, B. F. Spencer, and J. Ou, "A test method for damage diagnosis of suspension bridge suspender cables," *Computer-Aided Civil and Infrastructure Engineering*, vol. 30, no. 10, pp. 771–784, 2015.